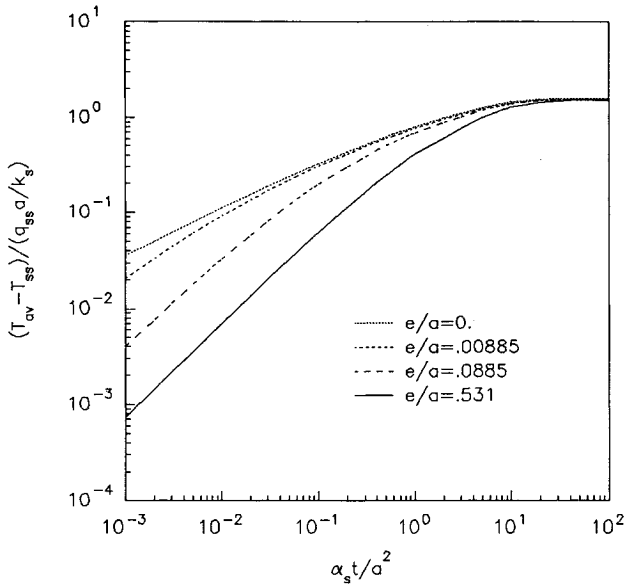

Fig. 2 Spatial average temperature of the sensor vs time for several values of hot-film thickness obtained from the USE simulation (β = 10,340/s, D/a = 4).

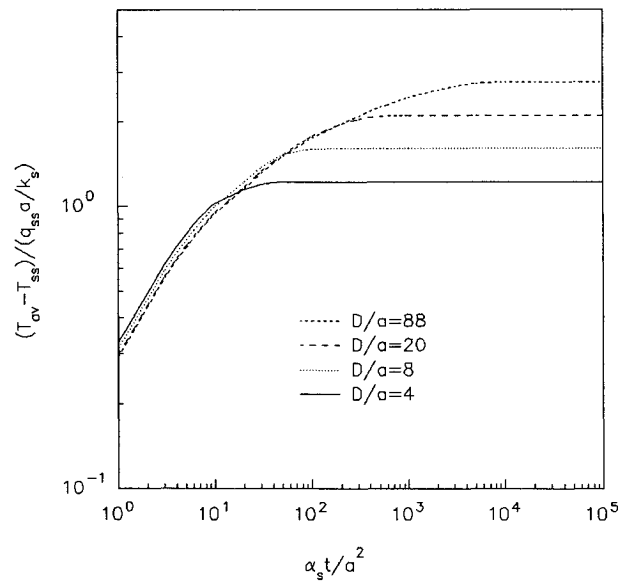

Fig. 3 Spatial average temperature of the sensor vs time for several values of substrate thickness obtained from the USE simulation (β = 10,340/s, e/a = 0.531).

Therefore, thermal storage in the hot-film sensor can be neglected for a thermal transient containing frequencies below approximately 40 Hz (corresponding to $t \approx 0.025$ s).

Figure 3 is a log-log plot of the spatial average temperature of the sensor vs time for several values of substrate thickness D/a. The numerical solution includes the heat loss through the electric leads. The ratio of the total heat lost to the electric leads to the total introduced heat, Q_l/Q_0 has the following values: 0.1977 (D/a = 4); 0.2390 (D/a = 8); 0.2748 (D/a = 20); 0.2910 (D/a = 88). The shift of each plot at small times, before steady state is reached, is caused by the different values of Q_l/Q_0. If the influence of Q_l were not included, Fig. 3 would be similar to the work done by Cole and Beck.[2] The D/a = 4 (thin substrate) case reaches steady state first with the lowest average temperature. The thicker substrate cases reach steady state at successively later times, each with a successively higher average temperature. The time to steady state can be estimated approximately by D^2/α_s, or by $t^+ = (D/a)^2$, since the heat transfer to the substrate dominates the time to reach steady state.

The transient computations were performed on a VAX 8800 computer using up to 35 surface elements in the substrate (14 on the hot-film) and an active interface of length of up to 281 times the hot-film size. Computation time for one run of the transient calculation was about 180 CPU s.

Conclusions

The constant-current responses of a thick hot-film sensor in steady airflow were computed by the USE method. Numerical results are in good agreement with the analytical solution for the spatial average temperature of the sensor at very early time. The heat storage in the metal sensor is important only at the beginning of the step response corresponding to higher frequency transients. Thus, the thermal storage in the thick hot-film sensor (e = 6 μm) may be neglected for a thermal transient containing frequencies approximately below 40 Hz. The time to steady state is controlled by the value of D, the effective substrate thickness, and not by the sensor thickness e, since the overall thermal mass is dominated by the substrate. Future research will include the analysis of airflow with an oscillating component.

References

[1]Schultz, D. L., and Jones, T. V., "Heat Transfer Research in Short Duration Hypersonic Facilities," AGARD AG-165, 1973.

[2]Cole, K. D., and Beck, J. V., "Conjugated Heat Transfer from a Strip Heater with the Unsteady Surface Element Method," *Journal of Thermophysics and Heat Transfer*, Vol. 1, No. 4, 1987, pp. 348–354.

[3]Park, C. H., and Cole, K. D., "Theory and Experiment for Metal-on-Polymer Shear Stress Sensor in Air Flow," *Proceedings of the American Society of Mechanical Engineering National Heat Transfer Conference* (Atlanta, GA), HTD-Vol. 249, 1993, pp. 61–71.

[4]Park, C. H., "Shear Stress Measurements with Metal-on-Polymer Shear Stress Sensor-Analysis and Experiment," Ph.D. Dissertation, Univ. of Nebraska, Lincoln, NE, 1994, pp. 71–78.

Unsteady Heat Transfer from a Sphere at Low Reynolds and Strouhal Numbers

Y. Bayazitoglu,* C. F. Anderson,† R. D. Cohen,‡ and R. W. Shampine†
Rice University, Houston, Texas 77251

Nomenclature

A_p = surface area of particle
D = particle diameter
k = thermal conductivity of the fluid
Nu_0 = steady Nusselt number at the acoustic Reynolds number

Presented as Paper 93-0915 at the AIAA 31st Aerospace Sciences Meeting, Reno, NV, Jan. 11–14, 1993; received Aug. 12, 1993; revision received Jan. 24, 1994; accepted for publication Jan. 26, 1994.

*Professor, Department of Mechanical Engineering and Materials Science, P.O. Box 1892. Member AIAA.
†Graduate Student, Department of Mechanical Engineering and Materials Science, P.O. Box 1892.
‡Associate Professor, Department of Mechanical Engineering and Materials Science, P.O. Box 1892.

$\hat{n}$ = unit surface normal
P = pressure
Pe = Peclet number, $U_a D/\alpha$
Re = acoustic Reynolds number, $U_a D/\nu$
S = Strouhal number, $\omega D/U_a$
U_a = acoustic velocity amplitude
α = thermal diffusivity
ν = kinematic viscosity
τ = nondimensionalized time, $t\omega/2\pi$
ω = angular frequency

Introduction

THE effect of a sound field in a fluid on the flow, and more recently on the heat and mass transfer for external flows, has been studied extensively. Of particular interest to this study is the effect of acoustics on a large field of particles. This is motivated by an interest in the effect of an intense acoustic field on combustion of pulverized coal particles.

Most of the work concerning acoustically driven external flows has been done in the domain of high Strouhal numbers, dealing primarily with the effects of acoustic streaming upon the flow. Recently, Gopinath and Mills[1] examined the effect of acoustic streaming upon the heat transfer from spheres at high Strouhal numbers.

By contrast, relatively little work has been done in the domain of low Strouhal numbers. Mori et al.[2] studied unsteady heat transfer from small isolated, spherical bodies at low Reynolds numbers. Larsen and Jensen[3] considered the evaporation rates of single droplets suspended in an unsteady flow. Ha[4] numerically studied heat transfer from a spherical particle in oscillating flow both with and without steady flow components.

In this study, we evaluate the flowfield and convective heat transfer rates for low Strouhal numbers for idealized uniform temperature spheres in a traveling sound wave using an axisymmetric formulation. We shall include the effects of temperature variable parameters for the fluid, as the problem of interest typically may vary over several hundreds of degrees. The problem is evaluated at Strouhal numbers of less than 1 for a range of small acoustic Reynolds numbers.

Governing Equations

We limit our analysis to cases where the particle is small compared with the acoustic wavelength and the particles are widely spaced. The gas in the Stokes layer near the particle can therefore be treated as incompressible, and we can consider an isolated, spherical particle at uniform temperature, instead of modeling the entire particle field. The surrounding fluid medium has temperature-dependent thermophysical properties. The nondimensionalized, differential governing equations for axisymmetric, incompressible flow and energy conservation are

$$\nabla \cdot \boldsymbol{u} = 0 \tag{1}$$

$$\frac{\partial u}{\partial \tau} + \boldsymbol{u} \cdot \nabla \boldsymbol{u} = -\nabla P + \frac{1}{Re} \nabla^2 \boldsymbol{u} \tag{2}$$

$$\frac{\partial T}{\partial \tau} + \boldsymbol{u} \cdot \nabla T = \frac{1}{Pe} \nabla^2 T \tag{3}$$

The boundary conditions which involve a uniform temperature sphere in a cooler medium with an acoustically induced velocity field are

$$\begin{aligned} u_r &= 0, \qquad u_z = 0 \\ T &= T_p \qquad \text{at} \qquad r = r_p,\ z = z_p \end{aligned} \tag{4}$$

where (r_p, z_p) represent the coordinates of the surface of the sphere and

$$\begin{aligned} u_r &= U_a \cos \tau, \qquad u_z = U_a \cos \tau \\ T &= T_\infty \qquad \text{as} \qquad r \to \infty,\ z \to \infty \end{aligned} \tag{5}$$

Implementation

Reynolds numbers considered by this study are too large for Stokes flow and too small for boundary-layer approximations to apply. Hence, the problem is treated numerically using FIDAP (FDI),[5] a general purpose computer program designed to model many classes of incompressible fluid flows. A freestream Prandtl number of 0.8005 and Strouhal numbers of 0.01 and 0.1 were considered for a range of acoustic Reynolds numbers from 0.5 to 15. Temperature variable parameters were implemented using set physical data points with linear interpolation between data points for all thermophysical parameters.

The numerical domain is an axisymmetric, rectangle, 12 particle diameters long and three and one-half particle diameters high. The finite element mesh has 1439 grid points and 360 quadratic elements. Steady-state results performed on this mesh are accurate to within 5% of standard correlations.[6] A convergence study sized the mesh for overall geometry vs accuracy, total mesh for computational time vs accuracy and mesh spacing over the domain. The numerical domain was verified for the transient case by lengthening the domain by 50% and alternately doubling the height with appropriate increases in mesh. Cases were rerun for the larger domains and those results correlated against the optimized domain results for a maximum error of 0.4%.

A velocity equal to the freestream velocity and temperature equal to the freestream temperature are imposed at the inlet section (the left wall). The freestream velocity is constant for the steady case and varying with "cos τ" for the transient case. A horizontal velocity equal to the freestream velocity and a uniform temperature equal to the freestream temperature are imposed on the top of the domain. The top of the domain has also been chosen far enough away, using the steady-state convergence study, so that a no-penetration condition (no velocity in the r direction) may be applied. The gradients normal to the wall of all primary variables are set to zero at the exit section (the right wall) modeling a fully developed flow. At the axis of rotation (the bottom wall) symmetry of both flow and temperature is applied. Thus, gradients of all primary variables are set to zero normal to the axis. On the surface of the sphere no-slip and no-penetration conditions are applied for velocity and the surface is specified at a constant temperature.

The solution procedure is to use the steady solution as an initial condition, then solve forwards using an implicit trapezoidal method until a quasisteady oscillation is observed. At each time step the transient solution is found using a quasi-Newton iteration method with Broyden's update (FDI).[5]

Results

A local surface average Nusselt number $Nu(t)$ is found by integral averaging of the nondimensional heat flux over the entire surface of the sphere, and a time-average Nusselt number Nu_t is found by integral averaging of the local surface average Nusselt number over one period, as follows:

$$\begin{aligned} Nu(t) &= \frac{1}{A_p} \int_{A_p} k \frac{\partial T}{\partial \hat{n}} \, dA \\ Nu_t &= \frac{1}{T} \int_0^T Nu(t) \, dt \end{aligned} \tag{6}$$

Mori[3] in an approximate analysis assumes the flow is quasisteady at low Strouhal numbers. This corresponds to a case where Strouhal number approaches zero and at every moment

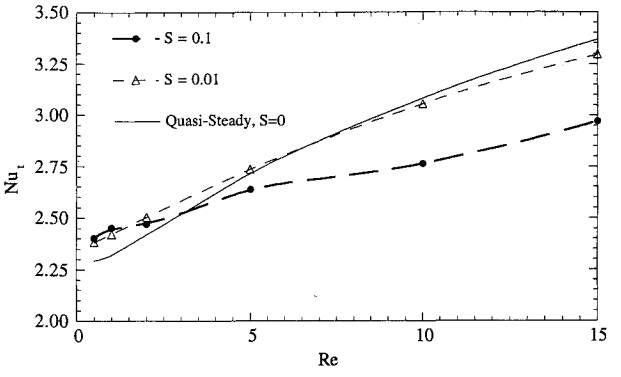

Fig. 1 Time-average Nusselt number Nu_t vs Reynolds number.

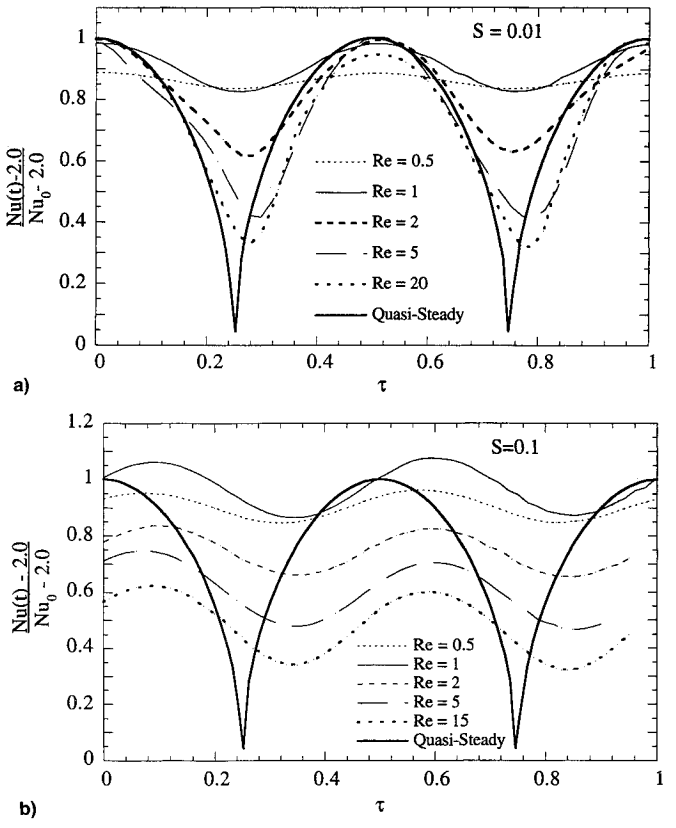

Fig. 2 Normalized Nusselt number $Nu(t)$ to Nu_0, ratio for Strouhal number: a) $S = 0.01$ and b) $S = 0.1$.

the steady state is considered to be instantly reached. The overall, or time-averaged Nusselt number is found for the quasisteady case by simply time-averaging the instantaneous results. The time-average Nusselt number for the two Strouhal number cases studied along with quasisteady-state results are shown in Fig. 1. The local surface average Nusselt number is shown in Figs. 2a and 2b, normalized with respect to a similar, steady convective transfer rate ($Nu_0 - 2.0$).[3,6] $Nu(t)$, varies smoothly and regularly with time, whereas oscillations of the local surface average Nusselt number vary with both Reynolds and Strouhal number. Values of Nu_t and the oscillation amplitudes of the local surface-average Nusselt number for the highest Reynolds number cases were compared with Ha[5] and found to be within 1–3%.

Discussion

For all cases studied, except for the quasisteady approximation, there is some phase lag between the flow oscillation and the temperature response. This thermal response, or thermal displacement, in turn, drives a phase lag in the heat transfer. The phase lag for $S = 0.01$ is small, but becomes more significant for the higher Strouhal number case, as shown in Figs. 2a and 2b. Thermal displacement translates at flow reversal to higher thermal gradients and greater heat transfer across portions of the sphere. Hence, even the lowest spatially averaged Nusselt number is significantly above the conduction limit of $Nu = 2.0$. Alternately, at times of maximum flow, thermal lag tends to insulate the sphere. The magnitude of thermal lag varies with both the Reynolds and the Strouhal number. Because the total thermal lag for the higher Strouhal number case is greater, the oscillations in local surface-average Nusselt number decrease at the higher Strouhal number.

Transient induced flows for many of the cases studied were quite small. However, the largest transient induced flow, found near the surface of the sphere at the highest Reynolds and Strouhal case, was over 30% of U_a. As the Reynolds and Strouhal number increased, transient flows also became more prominent.

It is necessary to assess how all these effects alter the time-averaged behavior. At lower Reynolds numbers, there are times when transience tends to increase the maximum heat transfer vs a quasisteady approximation. However, for the higher Reynolds number cases the heat transfer is consistently less than the quasisteady prediction. We clearly see in Fig. 1 that for the larger Reynolds number cases, heat transfer decreases as the Strouhal number increases. Furthermore, from Figs. 2a and 2b, oscillations in the local surface-average Nusselt number grow with Reynolds number. For Reynolds numbers on the order of unity, as the Strouhal number increases, the time and spatially averaged Nusselt number Nu_t rises, as shown clearly in Fig. 1. Thus, as convection becomes less important, transient phenomenon tend to increase heat transfer.

Conclusions

Using an existing finite element package this study has developed a model for transient analyses of this geometry. This model has a computational domain and boundary conditions shown to be acceptable for the determination of the transient Nusselt numbers for this study's range of interest.

This study has shown that a quasisteady approximation for Strouhal numbers for flow around a sphere, even for Strouhal numbers as low as 0.01, is incorrect. A quasisteady approximation yields conduction values at the flow reversal with very sharp decreases and increases in heat transfer. Time-dependent thermal displacement together with unsteady induced flows are found to significantly change the timewise behavior as well as the overall heat transfer vs a quasisteady approximation. As the Reynolds number rises transient response tends to insulate the sphere and the averaged Nusselt numbers decrease. Heat transfer decreases as the Strouhal number is increased for most of the range of Reynolds numbers studied. However, transient effects increase heat transfer in cases where $Re \sim 1$.

Acknowledgment

The authors would like to acknowledge the generous support of Texas THECB/ERAP Grant 003604-014.

References

[1]Gopinath, A., and Mills, A. F., "Convective Heat Transfer from a Sphere due to Acoustic Streaming," *Journal of Heat Transfer*, Vol. 115, No. 2, 1993, pp. 332–339.

[2]Mori, Y., Imbayashi, M., Hijikata, K., and Yoshida, Y., "Unsteady Heat and Mass Transfer from Spheres," *International Journal of Heat and Mass Transfer*, Vol. 12, 1969, pp. 571–585.

[3]Larsen, P. S., and Jensen, J. W., "Evaporation Rates of Drops in Forced Convection with Superimposed Transverse Sound Field," *International Journal of Heat and Mass Transfer*, Vol. 21, 1978, pp. 511–517.

[4]Ha, M. Y., "A Theoretical Study of Augmentation of Particle Combustion Via Acoustic Enhancement of Heat and Mass Transfer," Ph.D. Dissertation, Pennsylvania State Univ., College Park, PA, 1990.

[5]*FIDAP Manual, Revision 5, 1st Ed.*, Fluid Dynamics International, Evanston, IL, 1990.

[6]Ranz, W. E., and Marshall, W. R., "Evaporation from Drops," *Chemical Engineering Progress*, Vol. 48, 1952, pp. 141–146, 173–180.

DSMC- and BGK-Based Calculations for Return Flux Contamination of an Outgassing Spacecraft

Charles R. Justiz* and Ronald M. Sega†
NASA Johnson Space Center, Houston, Texas 77058
and
Charles Dalton‡ and Alex Ignatiev§
University of Houston, Houston, Texas 77204

Introduction

THE capability to predict contamination of a spacecraft surface is becoming an important design tool. In this study, the recontamination of a spacecraft surface, directly exposed to the ram flux, is examined. The specific problem to be considered assumes that a surface has been contaminated by a rocket plume and that, subsequent to the exposure, the contaminated surface is placed in the ram flux. Given a fixed desorption rate, recontamination of the surface by the return flux contact is calculated. The calculations are done using a BGK-based method, a direct simulation Monte Carlo (DSMC-) based method, and a full flow Monte Carlo (FFMC-) based method. Surface accommodation is included since an earlier investigation showed that it had a noticeable effect on the near-wake environment.[1] Of concern in this investigation is the level of contamination resulting from one contamination mechanism as predicted by the three computational schemes mentioned above.

Several observations by previous investigators[2–5] are relevant to the surface accommodation used in this study.

1) Molecules with large dipole moments (H_2O, CO_2, etc.) have relatively long interaction times (i.e., a few milliseconds) with a surface, thus allowing for more complete thermal accommodation with a surface. The result is diffuse emission patterns.

2) The engine molecular exhaust velocities are near 3500 m/s, and thus fall into the energy range where diffuse scattering from a surface is exhibited.[6]

3) The spacecraft surface can be described as rough, i.e., it has irregularities such as seams, penetrations, and tile cracks. These irregularities cause scattering to be diffuse. Contamination of a surface also causes specular scattering to become diffuse scattering due to the nonuniformity of surface deposits.

For the conditions just cited, the diffusely scattered molecules have velocities indicative of the surface temperature, which implies complete thermal accommodation.

Computational Investigation

The motivation for this study is to be able to predict certain flow phenomena for NASA missions such as the wake shield facility (WSF). The capability to predict surface contamination would be invaluable in assessing performance of the WSF.

The codes used in comparing computational capability are MOLFLUX,[6] a BGK-based code, and CARLOS,[7] which has the capability of serving as either a DSMC or a FFMC code. The computational investigation was composed of two parts. The first part was to compare the two codes, MOLFLUX and CARLOS (acting as a DSMC), for impacts of the ambient species with the disk surface. For our purposes, the ram flux is based on the 400-km species as presented by the 1976 U.S. Standard Atmosphere.

The second and major part was to calculate the return flux when a CO_2 outgas condition interacted with the ambient flow. There are several input parameters:

1) The disk is taken to be 10 m in diam, which is representative of a WSF.

2) The disk has a forward velocity of 7.7 km/s.

3) The altitude for the computation is 400 km.

4) The freestream number density is 2.09×10^8 particles/cm^3 with a freestream temperature of 1000 K.

5) In the outgassing part of the calculation, CO_2 was outgassed at a rate of 1.0×10^{-11} grams/cm^2/s uniformly over the surface, and the disk surface temperature of the spacecraft was maintained at 373 K.

Computational Results

The BGK-based MOLFLUX code was run to determine the number of surface impacts for the ambient species at 400 km for both reduced and full surface accommodation conditions. The peak value is uniformly distributed over the disk surface and is approximately 2.0×10^{14} impacts/cm^2/s for both surface conditions. The CARLOS code was also run for the full surface accommodation condition for the same ambient species conditions at 400 km. The results show that the surface collisions are uniformly distributed over the disk and the peak value is approximately 2.0×10^{14} impacts/cm^2/s, which is essentially the same as the BGK results. In comparing the results of the MOLFLUX runs, it is noted that there is virtually no difference in results for the two surface accommodation conditions. Therefore, the full physics representation was done only for the full surface accommodation conditions.

Since the main purpose of the investigation is to contrast the results of the full flow model and the BGK model for the

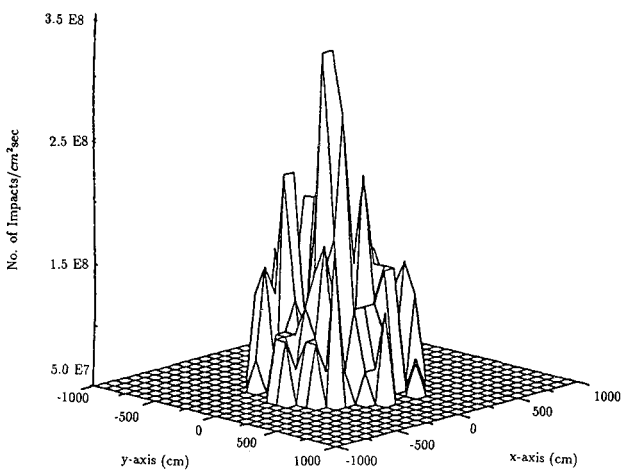

Fig. 1 Return flux impacts for outgassing species—BGK model—reduced surface accommodation.

Presented as Paper 93-0725 at the AIAA 31st Aerospace Sciences Meeting, Reno, NV, Jan. 11–14, 1993; received Aug. 12, 1993; revision received April 5, 1994; accepted for publication April 6, 1994.

*Research Pilot. Associate Fellow AIAA.
†Astronaut. Senior Member AIAA.
‡Associate Dean, Cullen College of Engineering. Associate Fellow AIAA.
§Director, Space Vacuum Epitaxy Center. Senior Member AIAA.